

# Thermal Management Technologies for Embedded Cooling Applications

Andrew Slippey, William G. Anderson, Michael C. Ellis, Clayton Hose, James Schmidt, and Jens Weyant  
Advanced Cooling Technologies, Inc.  
1046 New Holland Ave.  
Lancaster, PA, United States of America, 17601  
Email: Andy.Slippey@1-act.com

## ABSTRACT

Embedded computing systems used in many applications are trending toward higher heat fluxes and powers. As a result, the thermal resistance between the electronics and the heat sink must be reduced to keep the electronics temperature to acceptable levels. The thermal resistance path includes the thermal interface material, conduction card, wedge lock interface, and card cage wall. In addition, a vapor chamber may be included to transform high heat fluxes to a lower flux that the other components can handle. This paper outlines three passive thermal improvements which are easily integrated into systems: (1) A CTE matched, high-heat-flux vapor chamber that replaces an existing CuMo heat spreader resulting in a temperature reduction of 43°C at a heat flux of 520 W/cm<sup>2</sup>, (2) an improved wedge lock with two directions of expansion, cutting thermal resistance by one-third, by increasing the surface area for heat transfer and maximizing contact pressure, and (3) an improved thermal design for a composite box that integrates heat pipes to overcome the very low thermal conductivity of composites, typically 1 W/m K. When combined with heat pipes integrated into the conduction cards, they can provide a 3-4x increase in dissipated power.

**KEY WORDS:** thermal, embedded computing, heat pipe, electronics cooling, high thermal conductivity, vapor chamber, composite enclosures, wedge locks, high heat flux

## INTRODUCTION

Embedded computing systems used in many military and avionics applications are trending toward higher heat fluxes, and as a result performance is being hindered by thermal limitations. One method to reduce the temperature increase is to embed heat pipes into the conduction card, as well as in the chassis [1]. The increased effective conductivity lowers the temperature drop for a given power.

The paper discusses three additional passive thermal devices that can also be incorporated into embedded systems. The first is a Coefficient of Thermal Expansion (CTE) matched vapor chamber suitable for cooling high heat flux chips. The electronics can be directly mounted to the vapor chamber, which transforms the high heat flux into a much lower heat flux that can be handled by the rest of the system.

The second device is an improved wedge lock that expands in two directions, reducing the thermal resistance. Finally, a method has been developed to embed heat pipes into composite electronics boxes, overcoming their very low thermal conductivity, on the order of 1 W/m K.

## HIGH-HEAT-FLUX VAPOR CHAMBERS

As power modules continue to decrease in size while increasing in power capabilities, advanced thermal solutions are required to dissipate the increased amounts of waste heat. Increasing the ability to spread heat from a concentrated heat input area (device scale) to a larger heat dissipation area (heat sink) has the potential to significantly reduce the maximum temperature a device reaches during operation. Current power electronics packaging often limits the ability to realize the full potential of advanced power electronics diodes and MOSFETs, thus requiring them to be derated. The ability to more effectively remove the heat from the device allows a more reliable module that can operate closer to its rated conditions, and can reduce system size and weight.

This section focuses on the design, development, and demonstration of a CTE matched, high heat flux vapor chamber heat spreader utilizing advanced heat spreader technology previously developed at Advanced Cooling Technologies, Inc. (ACT) [2]. This is a passive packaging solution with built-in electrical isolation and the ability to act as a drop-in replacement for the current heat spreader.

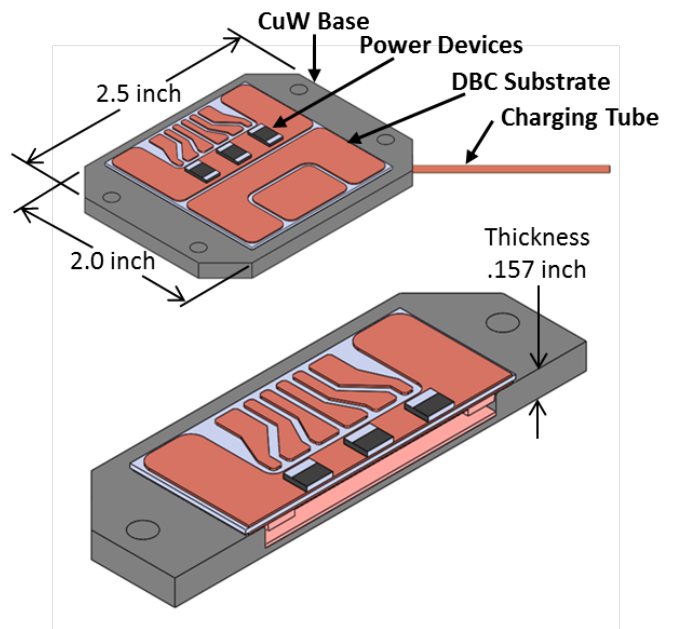


**Figure 1. 3D solid model (top) and cross-section (bottom) of high heat flux vapor chamber heat spreader.**

Advanced vapor chambers designed to dissipate heat in high flux regions have been built and tested in a laboratory environment achieving heat fluxes in excess of 700 W/cm<sup>2</sup> [3,4]. Specialized wick features within the vapor chamber

allow the working fluid within the vapor chamber to vaporize and flow more readily than standard vapor chamber designs [2].

**Design and Fabrication**

Figure 1 shows the 3D solid model of the high heat flux vapor chamber heat spreader with integral Direct Bond Copper (DBC) substrate and electrical devices attached.

The vapor chamber heat spreader was designed with a copper-tungsten (CuW) metal matrix composite single piece base onto which the DBC substrate is brazed. The base and DBC substrate have a copper powder wick attached prior to assembly to facilitate liquid working fluid flow to the heat input area. The porous structure of the wick and surface tension of the working fluid generate capillary pressure which acts to “pump” the condensed working fluid back to the heat input area where the working fluid is vaporized. The areas of wick under to the heat input areas have converging lateral arteries developed by ACT to accommodate the high input heat flux [2]. Figure 2(a and b) show trial vapor chamber components with attached wicks. Figure 2(c) shows the converging lateral arteries of a high heat flux vapor chamber wick. Bonding between the CuW base and DBC/wick was facilitated by metalizing the CuW base with copper. This metallization also provides a barrier between the working fluid and base material. Copper and water are known to be compatible, as their use in heat pipes is extensively documented [5]; however, insufficient compatibility data is currently available between water and tungsten. The CuW base also includes a central structural post to limit DBC deflection when the vapor chamber is evacuated and operating below 100°C. Once assembled, the vapor chamber had the electronic devices attached using high-temperature solder. With the devices attached, the vapor chamber was charged with the appropriate volume of water. Figure 2(d) shows the assembled CTE matched, high heat flux vapor chamber heat spreader.

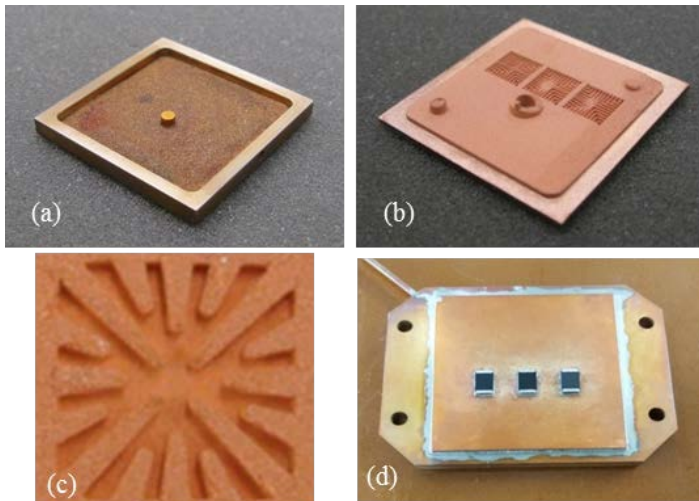


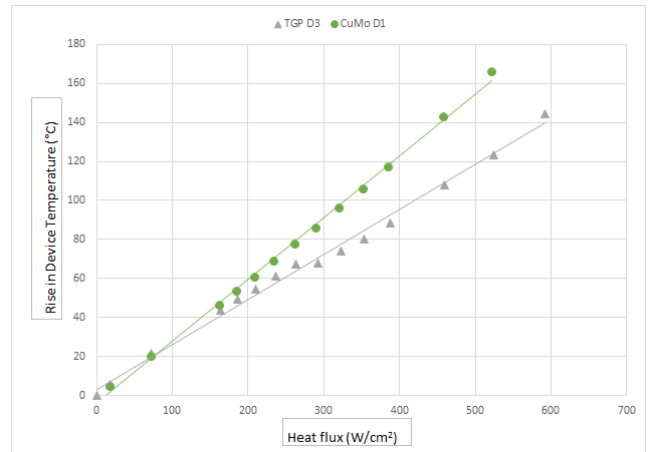
**Figure 2. (a) Copper plated trial CuW base with copper wick, (b) DBC with copper wick including high heat flux provisions, (c) converging lateral arteries of the high heat flux wick region, and (d) completed CTE matched, high heat flux vapor chamber heat spreader.**

**Vapor Chamber Experiments and Results**

An experimental setup was developed in order to investigate the performance of the vapor chamber heat spreader compared to a standard CuMo heat spreader. The heat spreaders were mounted on a liquid-cooled heatsink connected to a recirculating chiller which supplied water at an inlet temperature of 30°C.

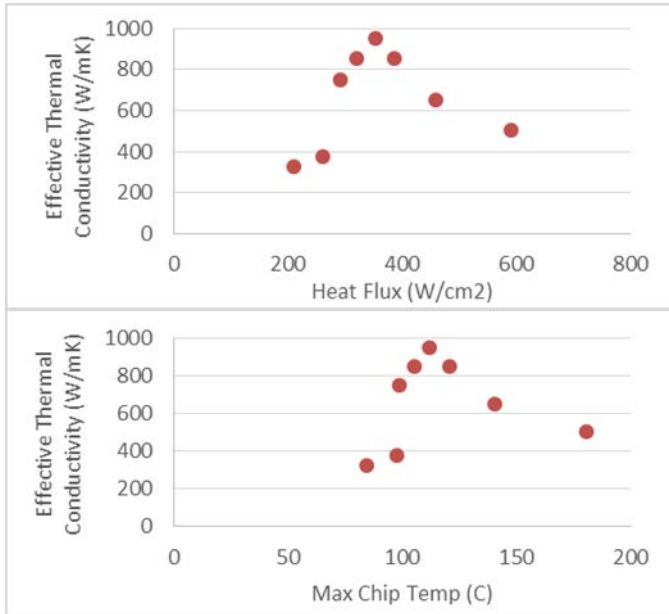
A DC power supply was used to apply power to 0.25 cm<sup>2</sup> ceramic chip resistors mounted on the heat spreaders. Prior to testing, the top surfaces of the modules were coated with boron nitride spray in order to provide uniform surface emissivity for IR imaging [6]. A FLIR A40 IR camera was used to measure the surface temperature of the device as well as several surrounding locations to further evaluate heat spreading performance for each module. After thermal equilibrium was achieved at each power level, the resistor temperature was recorded using the IR camera software. The heatsink outlet temperature was also recorded.

Figure 3 compares the temperature rise of the resistor in both heat spreaders. This plot shows that the performance of the vapor chamber heat spreader over the CuMo heat spreader becomes more and more pronounced with increasing heat flux. The measured average rise in device temperature of the vapor chamber device was 50 degrees lower than the CuMo resistor at this same heat flux.



**Figure 3. Comparison of the rise in chip resistor temperature for CuMo versus vapor chamber heat spreader over a range of heat fluxes.**

In order to quantify the performance improvement through the implementation of a vapor chamber heat spreader, a finite element analysis (FEA) using ANSYS was performed to determine the effective thermal conductivity required to match the experimental data. The results are shown in Figure 4 plotted against both heat flux and maximum chip temperature. The results show an effective thermal conductivity that peaks at 950 W/m-K, which occurs at a heat flux of 354 W/cm<sup>2</sup> and a maximum chip temperature of 112°C. This thermal conductivity is about 5 times better than standard heat spreader materials (CuMo, CuW, or AlSiC) and about 2.5 times better than copper.



**Figure 4. Vapor chamber heat spreader effective thermal conductivity as a function of heat flux (top) and maximum chip temperature (bottom).**

### ICE-LOK™ IMPROVED WEDGE LOCK

In the current state-of-the-art high-density electronics assemblies, slice-form electronics cards are fastened to chassis with embedded heat sinks by a wedge lock. This provides a separable mechanical connection that fixes the card in the chassis and provides a thermal path for heat rejection from the card; see Figure 5. The ease of integration and maintenance of these electronics packages has resulted in industry adoption of these assemblies and development of standardized chassis, card, and wedge lock dimensions [7]. Improving the thermal resistance of the wedge lock is key to improving the thermal performance of these systems.



**Figure 5. Typical conduction cooled card module, wedge lock, and chassis.**

As shown on the left in Figure 6, a conventional wedge lock expands in one direction to lock the card into the chassis. A new, improved wedge lock has been that enhances card-to-chassis conduction through making additional contact between the card conduction frame and the chassis guide faces; see the right in Figure 6. The Isothermal Card Edge Lok (ICE-Lok™) described below is wedge-type card retainer, but with the wedge faces cut at a compounded angle. When actuated, this allows the wedges to move with four degrees of freedom, expanding the card retainer in two, rather than a single direction; see Figure 7. L-brackets on the wedges contact the conduction card frame and tab, and form new paths for heat to reject through, increasing the overall surface area available for heat transfer, allowing the retainer to achieve a lower thermal resistance.

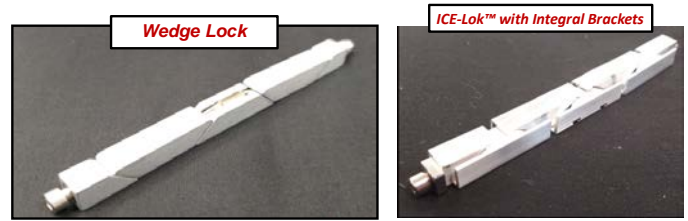


**Figure 6. A conventional wedge lock only expands in one direction, limiting the heat paths from the card to the sink. In contrast, the ICE-Lok™ has two directions of expansion, and an integral flange to reduce thermal resistance.**



**Figure 7. ICE-Lok™ expands in two directions when actuated.**

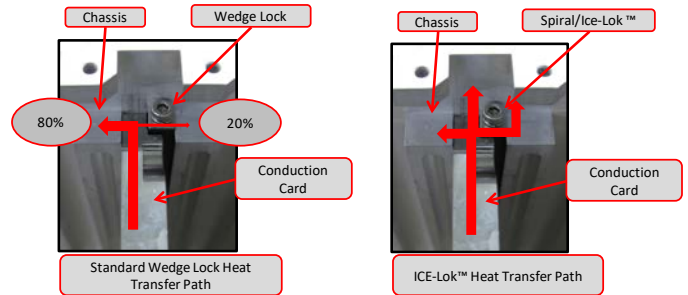


**Figure 8. Only 20% of the heat in a conventional wedge lock travels through the wedges. The ICE-Lok™ has improved heat transfer through the flanges, bypassing the wedges.**

As shown in Figure 8, the standard wedge lock expands in one direction and has a high thermal resistance, which results in two heat paths. Roughly 80% of the power travels through the card-chassis interface, while the remaining 20% of the power travels through the high-thermal-resistance wedge lock into the chassis.

In contrast, the ICE-Lok™ expands in two directions. The integral flanges provide two more low resistance heat paths, with heat traveling through both integral flanges.

### Qualification Testing

No industry standard qualification testing program currently exists for wedge lock devices used for military and spacecraft applications. In addition to thermal testing, ACT worked with Lockheed Martin Advanced Technology Laboratories to develop Thermal Cycling, Shock/Vibration, and Retention test procedures.

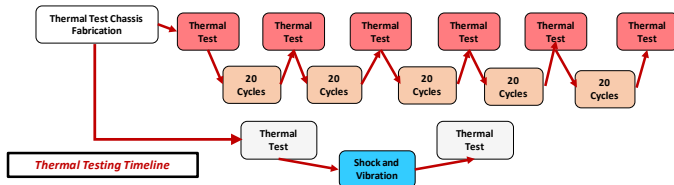


**Figure 9. ICE-Lok™ Thermal Cycling and Shock/Vibration Qualification Plans.**

The retention test showed no displacement when a 300-pound (1330 N) force was applied to attempt to remove the card. For shock/vibration testing, the parameters were chosen based on MIL-STD-810G Shock and MIL-STD-883 Vibration, which encompasses military aircraft, Delta IV, and Atlas V. No problems observed with the ICE-Lok™. The ICE-Lok™ survived the shock and vibration tests with no problems.

The thermal cycling test measured the degradation in thermal performance from beginning to end of life for the card, which was defined as 100 insertions & removals. As shown in Figure 9, the wedge lock was thermally tested at the beginning, and again after each additional 20 cycles. The results are shown in Figure 10. The ICE-Lok™ thermal resistance is roughly two-thirds of the resistance of competing high performance wedge locks.

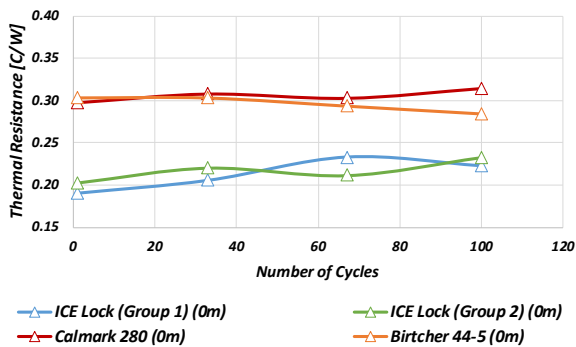


**Figure 10. Wedge lock thermal resistance versus number of cycles.**

### COMPOSITE BOXES WITH HEAT PIPES

Advanced materials such as carbon fiber reinforced polymer (CFRP) composite provide attractive structural solutions in applications where reducing mass is critical. The carbon fiber matrix of CFRP provides strength comparable to steel with only one quarter of the mass. Additionally, CFRP sheet can often also provide the required strength in a thinner form factor than comparable metals, further increasing the mass savings. However, the increased use of composites can cause thermal challenges. CFRP composites typically have a thermal conductivity on the order of 5 W/m-K [8], while carbon steel is near 50 W/m-K and aluminum is near 200 W/m-K. Traditional electronics enclosures made from metals double as physical structures and as heat spreaders that conduct heat away and over large surfaces, but composites act as thermal insulation. Heat generated by electronics causes internal temperatures to rise and has detrimental impact on the performance and reliability of those same electronics or others within the enclosure. ACT has demonstrated a method of using constant conductance heat pipes (CCHPs) that penetrate

through the CFRP walls to overcome these thermal limitations. The CCHPs transport significant heat energy through a limited cross-section with a minimal temperature penalty [9]. CCHPs are passive, two-phase, thermal transport devices which have effective thermal conductivities on the order of thousands of W/m-K. The heat pipes provide a high conductivity path for heat energy to pass from within the enclosure to outside the enclosure with minimal impact on the structural integrity of the wall. The CFRP is fabricated without changing the process or tooling and the pipes are embedded in a post-formation operation.

A light-weight CFRP enclosure was developed for the PC/104 form factor that is scalable for various embedded computing applications. PC/104 circuit cards stack vertically, each one plugging in to the next rather than each plugging into a single backplane. The enclosure design follows this stacking approach, so that the height of the box can be customized to match the cards included for the particular application. Each slice of the box consists of four CFRP walls and four corner pieces. Typically, one wall will have pass-through electrical connectors to attach input and output cables.

The thermal management system (TMS) designed to transport heat from within the enclosure through the poorly conductive CFRP walls to an external sink follows a modular approach just like the PC/104 cards and the enclosure design. The modular design allows the TMS to be included only where necessary, near components that dissipate significant power. The TMS may be inserted on one, two or three walls, depending on how much power is dissipated by the devices in that slice. In this way, excess mass of TMS is reduced when it is not necessary for a particular design. Mass of the TMS must be carefully considered, since weight reduction is the primary motivating factor for using CFRP.

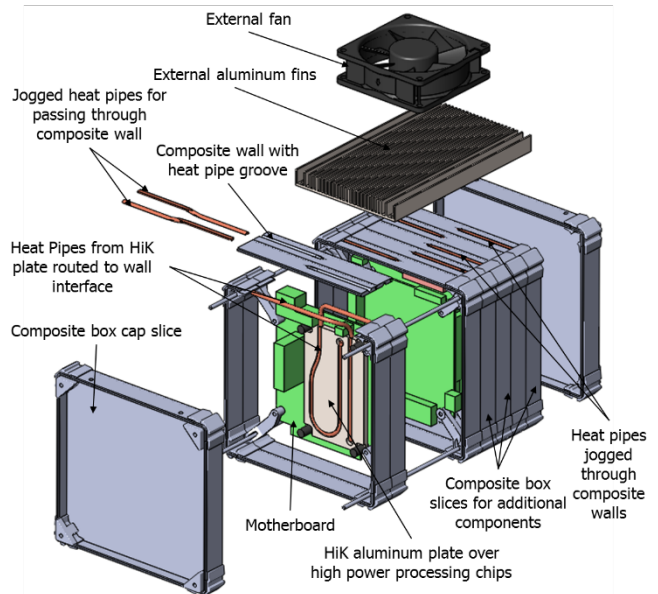


**Figure 11. Exploded view of CFRP enclosure with thermal management system.**

The CFRP enclosure's TMS consists of three subsystems. The first subsystem, inside the box, transports heat from the highest power chips to the walls. An aluminum plate with embedded CCHPs, called a HiK™ plate, replaces the fins and

a fan that would typically be attached to the motherboard processor. The CCHPs extend from this plate and are attached to the second subsystem on the walls of the box. The second subsystem is the critical link that transports heat through the composite walls. CCHPs, embedded in and jogged through the walls, collect heat from the inside of the box and transport it outside the box. CCHPs that are not directly coupled to a HiK™ plate may have fins attached on their interior surfaces to facilitate collecting the heat from the air within the box. The third subsystem is the external method for removing the heat to the ultimate sink. The testing demonstration uses an aluminum fin stack with a fan to reject the heat to air as the ultimate sink. These external fins could be switched out for a liquid-cooled cold plate, thermoelectrics, a natural convection fin stack, or some other interface to a larger system heat rejection system depending on the conditions and requirements of the actual application. If access to the internal electronics must be maintained, the slices cannot be permanently attached together. Thus, the external heat sink is designed to be removed and reattached easily, maintaining the modularity of the computer and enclosure design. Figure 11 shows the final design for CFRP enclosure and TMS demonstration unit.

### Design and Fabrication

CFD analysis was performed to assess the design's thermal performance in a natural convection case. Two baseline cases with no TMS were analyzed on a slice of the box. The first case is a CFRP box while the second case uses the same geometry but the material is changed to aluminum. The test case of the CFRP box with the TMS was then analyzed. The results for the test case show a 115 °C reduction in the maximum device temperature from the baseline CFRP case and a 96 °C reduction from the baseline aluminum case.

To fabricate the TMS, a procedure was developed to flatten and jog the CCHPs into an enclosure wall and embed them with epoxy. A sample wall with an embedded CCHP was repeatedly cycled back and forth from room temperature to over 100 °C. The epoxy exhibited no sign of cracking, peeling, or delamination after cycling. Also, the embedded CCHP was tested after cycling and confirmed that the pipe was a functioning heat pipe.

The CFRP pieces have a smooth surface finish straight out of the mold, and the corner pieces require no additional machining. When the wall sections are molded, they are extra-long and must be cut to length. Wall sections which will be included in the TMS require an additional machining operation to generate the appropriate groove geometry for embedding the through-wall jogged heat pipes.

Two complete CFRP enclosures were fabricated mounted with circuit boards to create two fully functional computers. There are six external electrical connectors, labeled in Figure 12, that interface with appropriate cables. Two thermocouples were also passed into the box for testing purposes. One thermocouple was attached to the HiK™ plate and the other was left to measure the internal air temperature around the center of the stack. The ambient external air temperature was also measured and recorded with a third thermocouple.

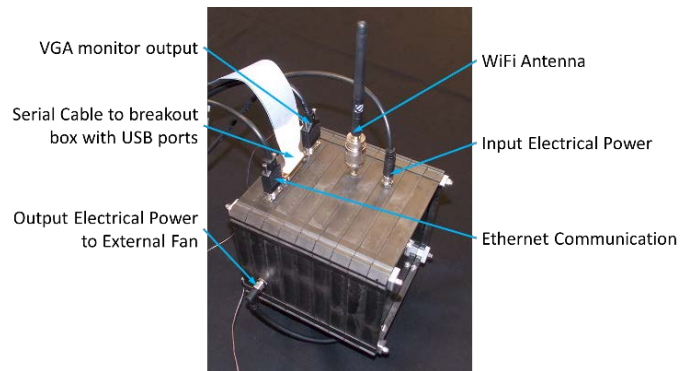


**Figure 12. Assembled CFRP Enclosure Showing External Electrical Connections on Side Opposite of the Thermal Solution.**

### Testing

Both prototype boxes were tested with the electronics and demonstrate that the TMS effectively and repeatably removes heat from the box. Results of a full power test of the CFRP enclosure are shown in Figure 13. After over an hour at nearly 100% processing load, the core temperatures reach a steady-state of 98 °C. Once the load is removed the temperatures quickly drop. There is a 76 °C temperature difference from the ambient room temperature of 22 °C to the core junction temperature. This difference is significantly larger than desirable. The internal air temperature never rises above 38 °C, maintaining an excellent 16 °C temperature difference to ambient. These results indicate that the through-wall heat pipes are effectively removing heat from the box, but the HiK plate is not properly removing heat from the motherboard chips to the walls. Additional testing confirmed that a flaw in the HiK™ plate design rendered it unable to dissipate the maximum power from the chips effectively, but when the heat is convected and spread to the internal copper fins of the other wall sections the thermal control is still sufficient. See [9] for more details about fabrication and testing of these prototypes.

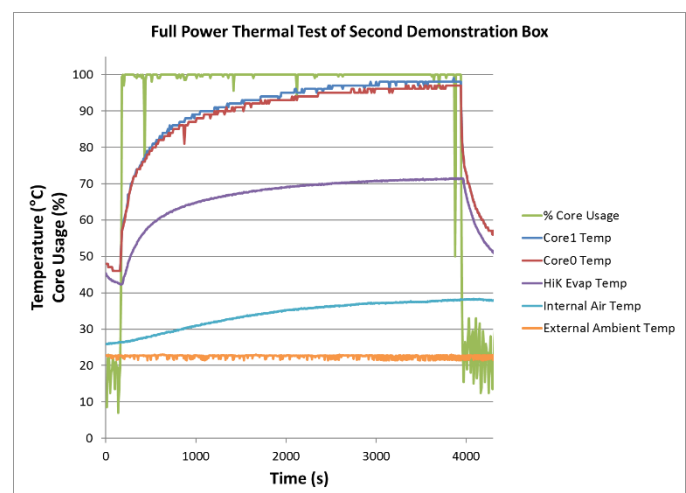


**Figure 13. Full Power Thermal Test Results for the Second PC/104 CFRP Enclosure Demonstration Box.**

## SUMMARY AND CONCLUSIONS

Embedded computing systems used in many applications are trending toward higher heat fluxes and powers. As a result, the thermal resistance between the electronics and the heat sink must be reduced to keep the electronics temperature to acceptable levels. This paper discusses three passive thermal improvements which are easily integrated into systems: (1) A CTE matched, high heat flux vapor chamber, (2) The Isothermal Card Edge Lok (ICE-Lok™) with two directions of expansion, cutting thermal resistance by one-third, and (3) an improved thermal design for a composite box that uses heat pipes to compensate for the very low composite thermal conductivity.

A CTE matched, high heat flux vapor chamber has been developed to meet the rising demands of power density and reliability in power electronics. The vapor chamber utilizes components that are well matched to the envelope material to reduce stress and improve reliability. The high heat flux handling capability of the vapor chamber heat spreader is made possible by the integration of a special wick structure beneath the critical heat flux areas. This wick is a mono-layer wick fed by converging lateral arteries. Modeling results based on the experimental data showed between a 2-5x increase in heat spreader thermal conductivity over a wide range of heat fluxes and operating temperatures. This work experimentally demonstrated the ability to replace an existing CuMo heat spreader with a passive drop-in replacement vapor chamber resulting in significant temperature reduction of 43°C at a heat flux of 520 W/cm<sup>2</sup>.

The ICE-Lok™ improves upon the current wedge lock, by redesigning the wedges to expand in two directions, as well as adding an integral flange. It can serve as a drop-in replacement card retainer for existing wedge locks, while reducing the thermal resistance by one-third. This reduces the temperature by 10°C for a card with 100W of power. Testing of the Spiral Lock over a 100-cycle lifetime, for both mechanical and thermal performance, in relevant environmental conditions has verified that the design of the retainer meets industry expectations of reliable performance in demanding environments.

Embedding heat pipes into a composite avionics enclosure demonstrates a method to overcome the primary weakness of composite structures: poor thermal conductivity. By embedding heat pipes in the composite structure and linking these heat pipes with finned, heat exchangers, component temperatures are maintained for a fully-functional avionics unit under 100% CPU load. This achievement has the potential to realize the benefits of composite structures' strength and weight improvements, without the typical poor thermal management drawback.

## Acknowledgments

The high-heat-flux vapor chambers was sponsored by the U.S. Army Research Laboratory under Cooperative Agreement Number W911NF-16-2-0047. The authors would like to thank Charles Scozzie, Damian Urciuoli, Nicholas

Jankowski, Darin Sharar, Claude Pullen, Michael Rego, Morris Berman, and Bruce Geil for their contributions to the vapor chamber work. The ICE-Lok™ was developed under AFRL Contract No. FA9453-15-C-0418. Brent Taft was the technical monitor, Jens Weyant was the PI, and James Schmidt and Matt Flannery worked on the program. The heat-pipe composite boxes were developed under AFRL contract FA8650-11-C-2183. ACT would like to thank Andrew Fleming, Cindy Obringer, Elizabeth Scherrer, Alexis Marruffo, and Anthony Puntel of AFRL for their support of this research.

## References

- [1] D. Campo, J. Weyant, and B. Muzyka, "A. B. Smith and C.D. Jones, "Enhancing Thermal Performance in Embedded Computing for Ruggedized Military and Avionics Applications," 2014 ITherm, Orlando, FL, May 27-30, 2014.
- [2] Ju, Y.S., Kaviani, M., Nam, Y., Sharratt, S., Hwang, G.S., Catton, I., Fleming, E., and Dussinger, P., 2013, "Planar vapor chamber with hybrid evaporator wicks for the thermal management of high-heat-flux and high-power optoelectronic devices," *Int. J. Heat Mass Transfer*, 60(1), pp. 163-169.
- [3] Kristen P. Bloschock ; Avram Bar-Cohen; Advanced thermal management technologies for defense electronics. Proc. SPIE 8405, Defense Transformation and Net-Centric Systems 2012, 84050I (May 3, 2012); doi:10.1117/12.924349.
- [4] A. Bar-Cohen, K. Matin, N.R. Jankowski, and D.J. Sharar, 2014, "Two-phase thermal ground planes: technology development and parametric results," *ASME Journal of Electronic Packaging*, 137 (1).
- [5] Kew, P. A., and Reay, D. A., 2006, *Heat Pipes*, Butterworth-Heinemann, Oxford.
- [6] Salem, T.E., Ibitayo, D., Geil, B.R., "Validation of Infrared Camera Thermal Measurements on High-Voltage Power Electronic Components", *IEEE Transactions on Instrumentation and Measurement* 56(5), 2007.
- [7] VITA Standards Organization. ANSI/VITA 48.0-2010, Mechanical Specification for Microcomputers Using Ruggedized Enhanced Design Implementation (REDI). 2010.
- [8] Shim, H.B., Seo, M.K., Park, S.J., "Thermal Conductivity and Mechanical Properties of Various Cross-section Types Carbon Fiber-reinforced Composites", *Journal of Materials Science*, vol 37. no 9. p 1881-1885. 2002 doi:10.1023/A:1014959603892.
- [9] Slippey, A., Ellis, M., Conway, B., Yun, H., "Heat Pipe Embedded Carbon Fiber Reinforced Polymer Composite Enclosures for Avionics Thermal Management." SAE 2014 Aerospace Systems and Technology Conference. Cincinnati, OH, 2014.